Comparison of Cold-Gas Simulations and Rocket-Launch Data for Constrictive Launchers

John J. Bertin*
The University of Texas at Austin, Austin, Texas
and
James L. Batson†
U.S. Army Missile Command, Huntsville, Ala.

Static-wall pressure distributions have been obtained during two flight test programs in which rockets were launched from constrictive tube launchers and a test program in which unheated air was exhausted through a stationary nozzle into constrictive tube launchers. The pressure measurements and the photographs of the tests clearly showed that, for some constrictive geometries, a significant fraction of the exhaust flow was turned upstream (i.e., became blow-by flow) as the exhaust either impinged directly on the constriction or was choked by the constriction. Even though the launchers in the flight-test programs were well instrumented, it was not possible to construct an exact flow model based solely on flight-test data. Using the data from the cold-gas tests, a realistic flow model was developed which explained the generation of blow-by flow. In addition, it was possible to correlate the nondimensionalized pressures (which were obtained by dividing static wall pressure by the "theoretical" value of the pressure downstream of the impingement shock wave) from the cold-gas tests with those of the rocket launchings.

Nomenclature

A_{aft} = cross-sectional area of the aft tube
A_{for} = cross-sectional area of the forward tube
$\dot{m}_{bb}$ = mass flow rate of the blow-by flow
$\dot{m}_{ex}$ = mass flow rate through the nozzle
p = static pressure
p_{t1} = total pressure in the rocket stagnation chamber
p_{t2} = total pressure downstream of a normal shock wave in the tube launcher
p_{2s} = static pressure downstream of a weak, impingement shock in the tube launcher
r_{ne} = exit-plane radius of the nozzle
x = axial distance with respect to the face of the step (or with respect to the departure edge)
x_{ne} = axial location of the nozzle-exit plane

Introduction

A variety of rockets are launched from "nontipoff" tubes, i.e., tubes which have a constrictive change in cross section. The cross section is varied so that the rocket is constrained immediately after ignition, but, once it has sufficient velocity, it flies free of any tube support for a short distance as it emerges from the tube. The complex flowfield that results when the rocket exhaust flow encounters the constrictive change in cross section may include significant blow-by flow, i.e., exhaust gases that are directed upstream into the annular region between the rocket and the launcher wall. Significant blow-by was observed during an eight-flight test program in which Rip-Zap configurations were launched from a sparsely instrumented, nontipoff launch tube. The constrictive launch tube, the launcher instrumentation, and the resultant data are described in Ref. 1.

Received Feb. 27, 1976; revision received July 6, 1976. This work was supported by the U.S. Army Missile Command through Contract DAAH01-C-1016.

Index categories: Jets, Wakes, and Viscid-Inviscid Flow Interactions; LV/M Configurations Design.

*Associate Professor, Department of Aerospace Engineering and Engineering Mechanics. Member AIAA.

†Engineer, U.S. Missile Research, Development and Engineering Laboratory. Member AIAA.

Additional tests were conducted to investigate the flow mechanisms responsible for the blow-by flow because of a concern for the possible generation of unbalanced forces that could influence the trajectory. Unheated nitrogen was exhausted from an underexpanded supersonic nozzle into a constrictive launch tube, which simulated only fraction of the length of the actual launcher. The objectives of these cold-gas tests conducted at the U.S. Army Missile Command included the determination of the effect of reservoir pressure, nozzle-exit position, and constrictive geometry on the blow-by mass-flow rate and on the static wall-pressure distribution in the launcher. When the exhaust flow impinged on the constriction, significant blow-by flow was generated. For many test conditions, the blow-by flow in the annular region between the rocket and the launcher wall was transonic.[2] In addition to these cold-gas tests, a four-flight test program was conducted in which Rip-Zap configurations were launched from a constrictive launch tube instrumented with static wall pressures, pitot pressures, and differential measurements from diametrically opposed static wall pressures. For the launcher geometries tested, the variations in the number of vent ports or in the geometry of the constriction had no significant effect on the static wall-pressure distributions[3].

Because of the complexity of the flow in the launcher, additional data were needed to construct a realistic flow model. A program was conducted in the University of Texas Rocket Exhaust Effects Facility in which unheated air was exhausted from an underexpanded, supersonic nozzle into a 0.2-scale model of the Rip-Zap launcher. Static wall-pressure distributions, pitot pressures obtained using a probe located in the annular region between the simulated rocket and the launcher walls (in order to measure the blow-by flow rate), and schlieren photographs were used to establish the flow mechanism responsible for the blow-by flow. Data were obtained over a wide range of reservoir pressure and of nozzle-exit position. During the course of this cold-gas test program, flight-test data were obtained which indicated that insignificant blow-by flow occurred for the Arrow configuration. Thus, the cold-gas experimental program was expanded to include the radius of the aft tube or, equivalently, the ratio of the aft-tube radius/ forward-tube radius as a variable.

Data from the cold-gas tests conducted in the University's Rocket Exhaust Effects Facility, from the Rip-Zap flight-test programs, and from the Arrow flight-test program are compared in the present paper. A primary objective of these correlations was to demonstrate the cold-gas simulations could be used to define the source of blow-by flow and the effect of the constrictive area ratio on the internal flow. In addition, the paper considers parameters that were not simulated properly in the scale-model cold-gas facility.

Test Programs

Static wall-pressure distributions and pitot pressures that were measured when an underexpanded, supersonic jet exhausted into a constrictive launcher are presented in the present paper. The parameters that characterize the supersonic exhaust flow were the half-angle of the conical nozzle, the nozzle exit radius, the throat radius, the ratio of specific heats, and the reservoir pressure. The geometric variables for the launcher configurations included the aft-tube radius, the forward-tube radius, the geometry of the constriction, the length of the forward tube, and the length of the aft tube. Over the range of values considered in the three test programs, the first two parameters, i.e., the aft-tube radius and the forward-tube radius, had the most significant effect on the flowfield. As will be discussed, viscous effects (which would depend on the length of the launcher) produced significant differences between the flight-test data and the cold-gas simulation in certain instances.

Rip-Zap Configuration

The overall length of the rocket assembly (which consisted of a 4:1 ogive forward section powered by a Zap motor) was 130.23 in. (330.78 cm). The outside diameter of the rocket was nominally 6.0 in. (15.2 cm). The launcher, which had an overall length of 148.60 in. (377.44 cm), consisted of two launch tubes that were assembled such that the aft tube had an inside diameter of 6.75 in. (17.15 cm) and the forward tube had an inside diameter of 8.75 in. (22.23 cm). Thus, the constrictive area ratio, i.e., A_{aft}/A_{for}, was 0.595. As shown in Fig. 1, two different geometries were used to accomplish the constrictive change in cross section. A modified rectangluar step was used for flights 9 and 10, whereas a 15° ramp was used for flights 11 and 12. To provide a reference for the reader, the location of orifice PS8 (the only gage in this region common to both geometries) is illustrated in Fig.1. The face of the rectangular step, which was 80.05 in. (203.33 cm) from the aft end of the launch tube, served as the origin for the dimensionless axial coordinate system, x/r_{ne}. Thus, as indicated in Fig. 1c, a negative value of the dimensionless axial coordinate corresponds to a location in the large-diameter forward tube of the launcher.

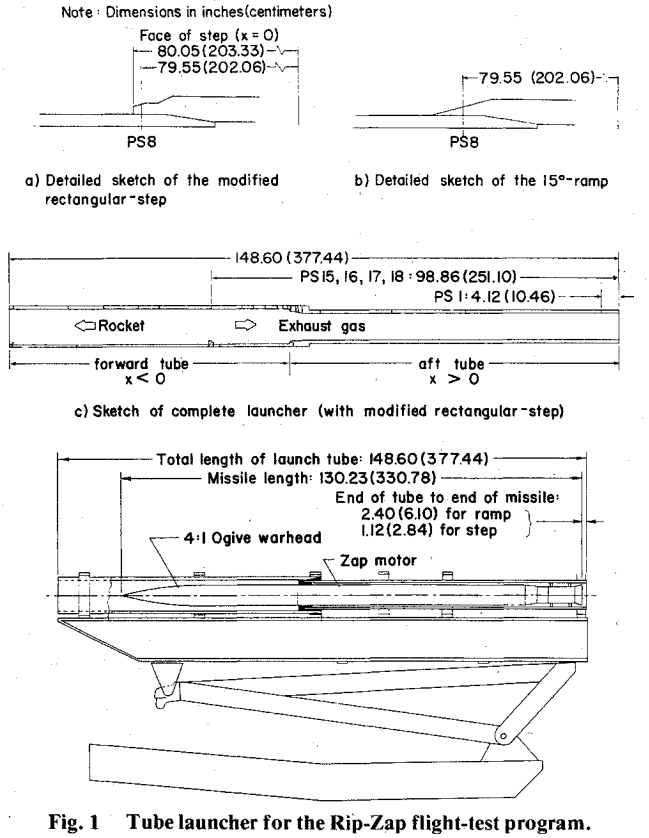

Fig. 1 Tube launcher for the Rip-Zap flight-test program.

The rocket gases, for which γ was approximately 1.18, exhausted from a conical nozzle having a half-angle of 10°22′. The reservoir pressure was approximately 1400 psi (9.66×10^6 N/m^2). The throat radius was 1.545 in. (3.924 cm), and the nozzle-exit radius was 2.833 in. (7.196 cm).

Arrow Configuration

The overall length of the rocket assembly was 65.66 in. (166.77 cm). The forward section of the Arrow configuration was 4.50 in. (11.43 cm) in diameter, whereas the diameter of the motor case was 3.80 in. (9.65 cm). The geometry of the constrictive, nontipoff launcher is illustrated in Fig.2. The small-diameter aft tube had an inside diameter of 3.86 in. (9.80 cm) and was 33.63 in. (85.42 cm) long. The large-diameter forward tube had an inside diameter of 4.56 in. (11.58 cm) and was 33.48 in. (85.04 cm) long. Therefore, the constrictive area ratio was 0.717. The change in cross section was accomplished by a 4° ramp. As noted in Fig. 2, the departure edge served as the origin for the dimensionless axial coordinate system, x/r_{ne}.

The rocket gases, for which γ was approximately 1.18, exhausted from a conical nozzle having a half-angle of pressure was approximately 1300 psia (8.97×10^6 N/m^2); the throat radius was 0.6676 in. (1.70 cm); and the nozzle exit radius was 1.4842 in.(3.77 cm).

Rocket Exhaust Effects Facility

Unheated air, for which γ was 1.4, exhausted from a convergent/divergent nozzle. The throat radius was 0.38 in. (0.95 cm), the nozzle-exit radius was 0.565 in. (1.44 cm), and the half-angle of the conical nozzle was 10°. Data are presented for reservoir stagnation pressures from 240 psia (1.66×10^6 N/m^2) to 1000 psia (6.90×10^6 N/m^2). Thus, assuming isentropic flow in the nozzle, the theoretical value of the static pressure in the nozzle-exit plane for the lower reservoir pressure was only slightly greater than the atmospheric value.

The instrumented, variable-area launch tube could be moved axially to vary the location of the nozzle-exit plane

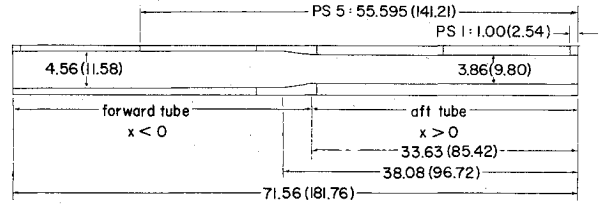

Fig. 2 Tube launcher for the Arrow flight-test program. All dimensions in inches (cm).

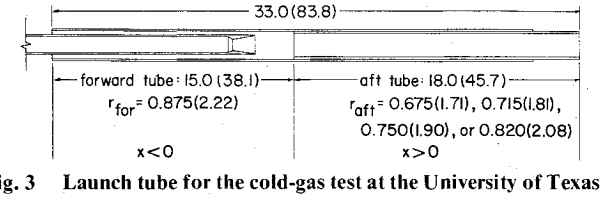

Fig. 3 Launch tube for the cold-gas test at the University of Texas at Austin. All dimensions in inches (cm).

relative to the constriction and, thereby, to simulate (in a quasisteady manner) the flowfields that result when the rocket accelerates through the launcher. The assumption that the exhaust flow for the dynamic rocket launching was quasisteady was based on the fact that the velocity of the exhaust gas was more than 20 times the velocity of the rocket as it left the launcher. Four launch tubes were used in the program so that, by varying the radius of the aft tube, the effect of the constrictive area ratio could be studied. As illustrated by the sketch of Fig.3, the overall length of the launcher was approximately 33.0 in. (83.8 cm). The large-diameter forward tube, which was approximately 15.0 in. (38.1 cm) long, was 1.75 in. (4.45 cm) in diameter. The aft tube, which was approximately 18.0 in. (45.7 cm), was either 1.35 in. (3.43 cm), 1.43 in. (3.63 cm), 150 in. (3.81 cm), or 1.64 in. (4.17 cm) in diameter. The change in cross section was accomplished by a rectangular step, which served as the origin for the dimensionless axial coordinate system.

Discussion of Results

To compare the data from the different test flights for a configuration, the static pressure measurements for a particular gage have been presented as a function of the nozzle-exit location instead of time. A curve fit of the observed position history for each flight was used to determine the time that corresponded to a particular location of the nozzle-exit plane. The nondimensionalized pressure data for selected gages for the Rip-Zap configuration were presented in Ref. 3 and for the Arrow configuration are presented in Figs. 9 and 10 as a function of the nozzle position relative to the origin of the axial coordinate system, x_{ne}/r_{ne}. This position parameter was positive when the nozzle-exit plane was in the small-diameter aft tube and was negative when in the large-diameter forward tube. Thus, as time increased, the nozzle-exit parameter x_{ne}/r_{ne} decreased from large positive values through zero and then to negative values. The static pressures recorded by all of the gages when the nozzle-exit plane is at a location (x_{ne}/r_{ne}) of interest can be presented as a function of the locations of the orifices x/r_{ne} to generate the launcher pressure distributions (e.g., Figs. 6, 7, and 11 for the flight tests).

Since the pressure measurements from the Rip-Zap flight-test program have been discussed previous[3], they only will be reviewed herein. When the rocket exhausted directly into the aft tube, the static pressures recorded by gages downstream of the nozzle-exit plane periodically rose suddenly and then decreased gradually. The pressure data indicated that the exhaust flow was fully supersonic. As the exit plane of the rocket nozzle entered the large-diameter forward tube, the static pressures increased suddenly (both for gages in the aft tube, e.g., PS1 of Fig. 1, and for gages in the forward tube, e.g., PS15 of Fig. 1). The magnitudes of the pressures were the same whether the exhaust flow encountered the modified rectangular step (flights 9 and 10) or the 15° ramp (flight 11). When the rocket exhausted into the forward tube, the static pressures recorded by gages that were downstream of the nozzle-exit plane (but in the forward tube) were more than twice the theoretical value of the pressure just downstream of a weak shock wave. Thus, it was apparent that a strong shock wave was generated when the rocket exhaust encountered the constriction. Correlations with the initial data from the cold-gas tests contributed significantly to recognizing that the flow downstream of the impingement shock wave was subsonic.

The static wall-pressure distributions obtained when unheated air exhausted into the 0.2-scale Rip-Zap launcher configuration are presented in Fig. 4. The dimensionless value

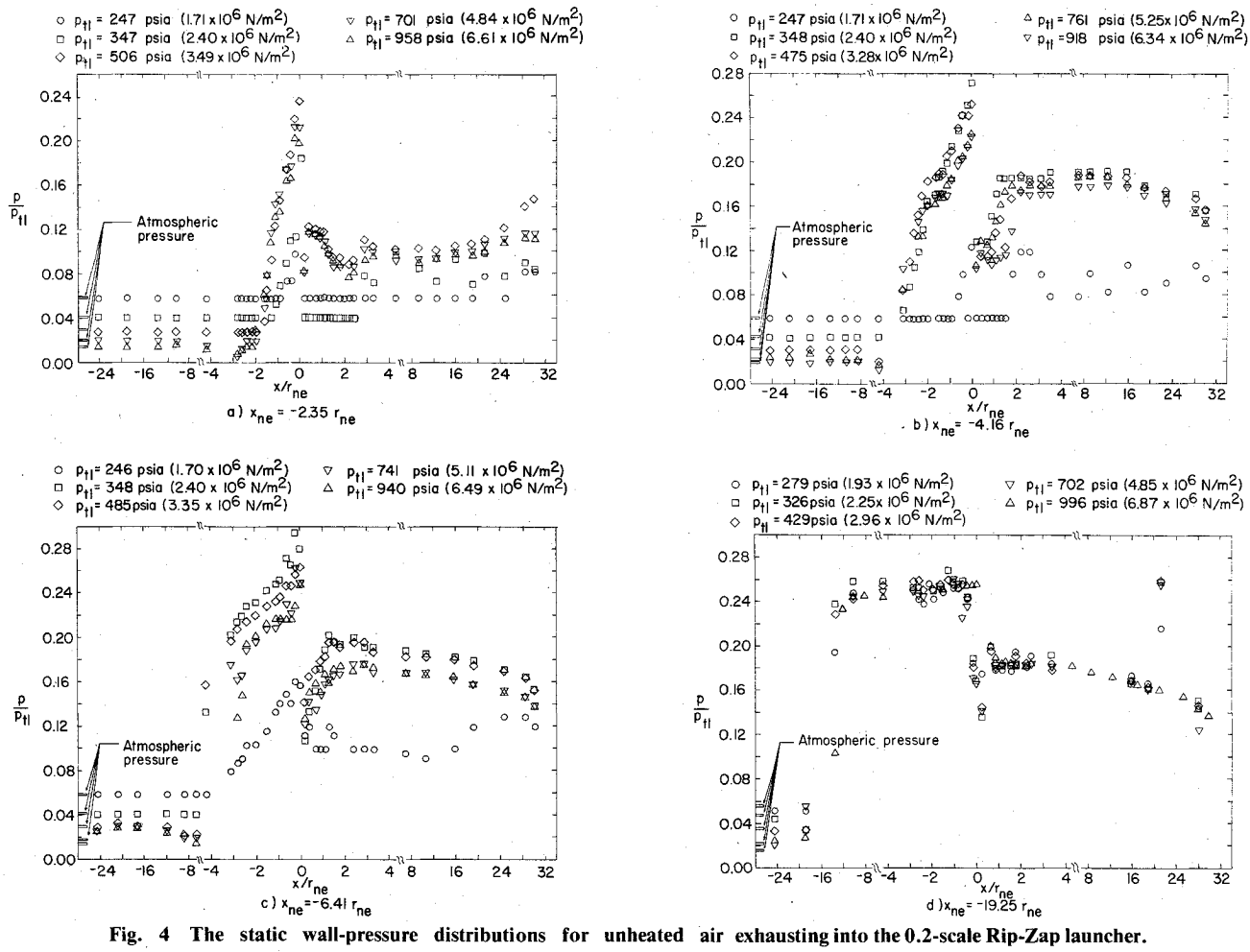

Fig. 4 The static wall-pressure distributions for unheated air exhausting into the 0.2-scale Rip-Zap launcher.

of the atmospheric pressure is designated by the bar symbol at the forward end of the launcher. A bar is included for each value of the stagnation pressure. To relate the symbol to the appropriate value of the stagnation pressure, note that p_{atm}/p_{t1} decreased monotonically as p_{t1} increased. Since the blow-by flow rate was sensitive both to the nozzle position and to the reservoir pressure when the nozzle-exit plane was located in the large-diameter forward tube, data illustrating the various flowfields are presented in Fig. 4.

The pressure distributions for $x_{ne} = -2.35\ r_{ne}$ are presented in Fig. 4a. For $p_{t1} = 247$ psia (1.71×10^6 N/m^2), the static wall pressure increased in the streamwise direction, reaching a peak at the base of the step. Downstream of the step, the static wall pressure was essentially constant for approximately $20r_{ne}$ into the small-diameter aft tube. The streamwise pressure variations for $x > 20r_{ne}$ indicate the occurrence of shock waves. Consider the following flow model as a possible explanation of these data. The theoretial value of the static pressure in the nozzle-exit plane (assuming isentropic flow in the nozzle) was only slightly greater than the atmospheric value. Thus, at this relatively low stagnation pressure, the central core of the exhaust flow did not impinge on the wall of the large-diameter forward tube. However, some of the fluid near the jet boundary apparently impinged on the face of the step, producing the pressure increase evident at the base of the step. The resultant pressure gradient from $x = 0$ to the forward end of the launcher ($x = -26.97\ r_{ne}$) was not sufficient to produce measurable blow-by flow. The constant pressures downstream of the step ($0 < x < +20\ r_{ne}$) indicate that the core of the supersonic exhaust continued to flow shock-free for a considerable distance down the aft tube. The viscous layer surrounding the jet attached to the wall and served as the wall boundary layer, becoming thicker with distance. The displacement effect of the boundary layer reduced the effective cross section of the aft tube until finally shock waves formed in the region $20\ r_{ne} < x < 30\ r_{ne}$. The essential features of the flow in the aft tube are believed to be similar to those described by Shapiro[4] for supersonic flow in a long duct with friction.

The general characteristics of the static wall-pressure distribution for $p_{t1} = 347$ psia (2.40×10^6 N/m^2) were similar to those described previously. Because the stagnation pressure increased, the pressure in the nozzle-exit plane increased, and the exhaust flow expanded through a greater angle as it left the nozzle. Therefore, at this reservoir pressure, the exhaust flow more fully filled the launcher. As a result, the supersonic flow proceeded only 2.5 r_{ne} into the aft tube before the effects of friction produced shock waves, as indicated in the streamwise pressure variation.

For $p_{t1} \geq 506$ psia (3.49×10^6 N/m^2), the pressure in the exit plane of the nozzle was so much greater than the atmospheric value that the exhaust flow impinged on the wall as it expanded into the forward tube. Downstream of the impingement shock, the pressure increased, reaching a maximum at the base of the step. Thus, the impinging exhaust flow encountered a large adverse pressure gradient that caused a significant portion of the exhaust flow to be turned upstream, i.e., to be reversed. The mass flow rate of the reverse, or blow-by, flow was approximately 8% of the mass flow rate through the nozzle. The blow-by flow rate was sufficient to produce nonatmospheric values for the static wall-pressure measurements in the annular region between the rocket and the wall of the forward tube. However, since the reverse flow was subsonic, the static pressure at the forward end of the annular region was equal to the atmospheric value. The experimental static pressures from the aft tubes are significantly less than the values obtained in tests where the aft-tube flow was subsonic, e.g., Fig. 4d. Thus, it is believed that the flow in the aft tube was supersonic over the entire range of p_{t1} for $x_{ne} = -2.35\ r_{ne}$.

The static wall-pressure distributions for $x_{ne} = -4.16\ r_{ne}$ are presented in Fig. 4b. For $p_{t1} = 247$ psia (1.71×10^6 N/m^2), the static pressure in the nozzle-exit plane was roughly equal to the back pressure (which, in the absence of significant blow-by flow, was equal to the atmospheric value). Thus, only fluid near the boundary of the exhaust flow was affected by the presence of the step. The impingement of the flow on the face of the step produced a local increase (of relatively small magnitude) in the static pressure for $-1\ r_{ne} < x < 0$. The resultant pressure gradient in the annular region was apparently insufficient to produce measurable blow-by flow. Just downstream of the step (in the region $0 \leq x \leq 1.5r_{ne}$), the pressure was constant. The core of the exhaust flow proceeded shock-free into the aft tube. The streamwise pressure variations for $x > 1.5r_{ne}$ are attributed to interactions between the viscous boundary layer and the shock waves induced by the presence of the boundary layer.

As the reservoir pressure was increased, radical changes occured in the flowfield in the launcher. The static pressure in the nozzle-exit plane (and the mass flow rate through the nozzle) increased in direct proportion to the reservoir pressure. Thus, as p_{t1} increased, the underexpanded nozzle flow had to turn through a larger expansion angle in order to satisfy the physical requirement that the pressure along the jet boundary be equal to the back pressure (i.e, the pressure is constant across a fluid/fluid interface). As the expansion angle increased, the impingement location moved further upstream. This movement is evident in the pressures measured at $x = -3r_{ne}$ (see Fig. 4b).

As a result of the changes in the mass flow rate, in the strength of the impingement shock, and in the fluid properties downstream of the impingement shock wave, the flow was choked by the constriction. A strong shock wave was generated in the region where the exhaust flow impinged on the wall. The fact that the static pressure decreased as the flow passed through the constriction indicated that the flow downstream of the impingement shock wave was subsonic. Recall that, if $dA < 0$, subsonic flow accelerates, whereas supersonic flow decelerates. The interaction between the strong shock wave and the exhaust flow created a large pressure gradient that caused a large fraction of the flow to be turned upstream. Thus, for $x_{ne} = -4.16\ r_{ne}$, an almost discontinous change in the blow-by flow rate occurred as the reservoir pressure was increased.

In the aft tube, the static wall pressure increased with distance from $x = 0$ to $x = r_{ne}$. As the flow accelerated past the step, the streamlines near the wall had small radii of curvature. The highly curved streamlines produced a large pressure gradient normal to the surface. Therefore, the wall-pressure measurements are believes to be significantly less than the static pressure of the fluid near the centerline of the tube. For $x > 2r_{ne}$, the static pressure decreased with distance, as would be expected in a flow where the viscous boundary layer caused the subsonic flow to accelerate in the "constant-area" aft tube. Thus, the static-pressure measurements downstream of $x = 2r_{ne}$ were consistant with the proposed flow model.

In addition to the marked changes in the static wall-pressure distributions and in the blow-by mass flow rate, there were other indications of the flowfield change. The audible characteristics of the noise produced during the operation of the facility also changed radically. As the stagnation pressure was increased and the shock pattern changed from mulitple, weak shock waves along the launcher to a single, strong shock wave in the forward tube, the noise generated by the flow in the launcher changed in pitch and in intensity.

A sketch of the proposed flow model for the choked flow is presented in Fig. 5. The relative dimensions of nozzle-exit radius (r_{ne})/aft-tube radius (r_{aft})/forward-tube radius (r_{for}) are to scale. The axial dimensions are not to scale. The pressure data clearly indicated that the impingement shock wave was normal. However, it was not possible to define in detail the oblique shock waves associated with the initial turning and deceleration of the exhaust flow. The extent over

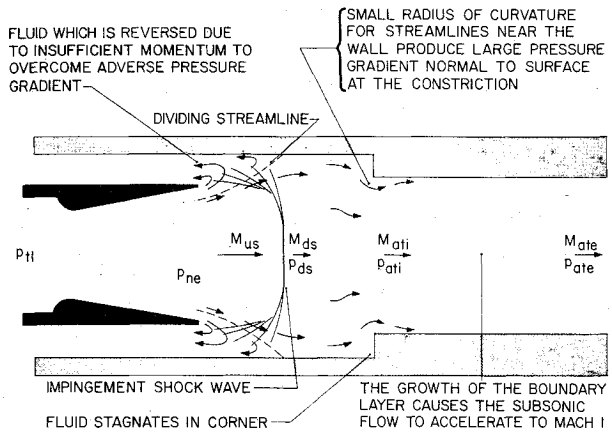

Fig. 5 A sketch of the proposed flow model for the choked exhaust flow in the constrictive launcher.

which the pressure rise occurred would be a measure of the interaction between the viscous shear layer and the complex shock-wave structure. The essential features of the flow model include 1) the underexpanded flow in the nozzle-exit plane (designed by the subscript *ne*), 2) the supersonic flow just upstream of the impingement shock wave (designated by the subscript *us*), 3) the subsonic flow just downstream of the strong impingement shock wave (designated by the subscript *ds*), 4) the reverse, or blow-by, flow (i.e., that fluid that cannot overcome the adverse pressure gradient generated by the flow impingement), 5) the region at the base of the step where some of the fluid that has passed through the shock system stagnates, 6) the subsonic flow at the entrance of the small-diameter aft tube (designated by the subscript *ati*), and 7) the sonic flow at the exit plane of the small-diameter aft tube (designated by the subscript *ate*).

To substantiate the validity of the flow model for the choked flow, let us compare the experimental pressures of Figs. 4c and 4d with the corresponding theoretical values. The theoretical values assume a one-dimensional flow incorporating the phenomena of Fig. 5 and use the relations of Ref. 5. The one dimensional exhaust flow was assumed to accelerate isentropically from the sonic conditions at the throat of the nozzle to the conditions just upstream of the shock. Since A_{for} was $5.302A^*$, M_{us} was 3.237. Downstream of the normal shock wave, the theoretical Mach number (M_{ds}) was 0.4626, and the theoretical static pressure (p_{ds}) was 0.2310 p_{t1}. The theoretical value for the static pressure was in good agreement with the experimental values of Figs. 4c and 4d. (The experimental values were approximately 0.22 p_{t1}.) The theoretical stagnation pressure downstream of a normal shock wave (0.2676 p_{t1}) was in good agreement with the pressures measured at the base of the rectangular step. Thus, 1) there was good agreement between the experimental data and the theoretical values (even for the relatively crude approximations), 2) the location of the normal shock wave was fixed with respect to the nozzle-exit plane, and 3) the choked blow-by flow rate was independent of nozzle-exit location (as will be shown in Fig. 8). These three observations support the conclusion (as illustrated in Fig. 5) that the fluid that constituted the blow-by flow did not pass through the shock system.

The pressure data indicated that the flow accelerated through the constriction (and was, therefore, subsonic). The subsonic flow immediately downstream of the shock wave in the forward tube ($M_{ds}=0.4626$) would accelerate to sonic conditions at the constriction, or "second-throat," if A were 0.7048 A_{for} (for a one-dimensional, isentropic flow). But A_{aft} was only 0.595 A_{for}. Thus, the aft tube was substantially smaller in cross section than the sonic throat area for the shocked flow. Once the critical value of reservoir pressure (or mass flow rate) had been exceeded, the large reduction in area (from A_{for} to A_{aft}) caused the flow to choke at the constriction. (The reader is reminded that other parameters, such as the characteristics of the shock impingement, are of extreme importance. In analyzing the Rip-Zap flight test data, the apparently anomalous behavior of the flight 12 data was attributed to probable "differences in the plume characteristics", see Ref. 3.) Adjustments took place in the internal flowfield, so that the flow in the exit plane of the aft tube was sonic, i.e., $M_{ate}=1$. The model for the resultant flow in the aft tube is that described by Shapiro[4] as choking due to friction. That the flow in the exit plane of the aft tube was indeed sonic was indicated by the static pressure measurements (see Figs. 4c and 4d). Assuming that the fluid near the center of the launcher accelerated isentropically from the *ds* conditions, the static pressure at the sonic location would have been 0.5283 p_{t2}. or 0.1414 p_{t1}. This value for the theoretical static pressure at the sonic location was essentially equal to the static pressure measurements from near the exit plane of the aft tube. Since the flow in the aft tube choked due to friction, it is necessary to simulate properly the length of the aft tube in the cold-gas tests.

The cold-gas simulations not only provided a realistic flow model that could be used to interpret the flight-test data, but the cold-gas pressure measurements correlated reasonably well with the flight measurements. The static wall-pressure distributions for $x_{ne} \approx -2.4\ r_{ne}$ are presented in Fig. 6. As noted in the section "Test Programs" the stagnation pressure for the Rip-Zap configuration was approximately 1400 psia (9.66×10^6 N/m^2). Therefore, only the cold-gas pressures for the highest reservoir pressure, i.e., 958 psia (6.61×10^6 N/m^2), are presented. In order to minimize the effect of γ on the data, the experimentally determined static wall pressures have been divided by p_{2s}, the theoretical value of the static pressure just downstream of a weak, oblique shock wave for the exhaust flow impinging on the forward-tube wall. The data from the dynamic rocket launchings were in good agreement with the data from the cold-gas tests in which the nozzle was stationary. As noted earlier, the assumption that the exhaust flow was quasisteady has been verified previously[6]. However, the correlation between the hot-gas data and the cold-gas data was surprisingly close in view of the differences between the flight data and theory.

The data obtained during the cold-gas test program clearly indicate that, when the exit plane of the nozzle was well into the forward tube, the exhaust flow was choked by the constriction,and the impingement shock wave was strong, i.e., normal to the axis of the launcher. Therefore, the experimentally determined static wall pressures have been divided by p_{t2}, the theoretical value of the stagnation pressure

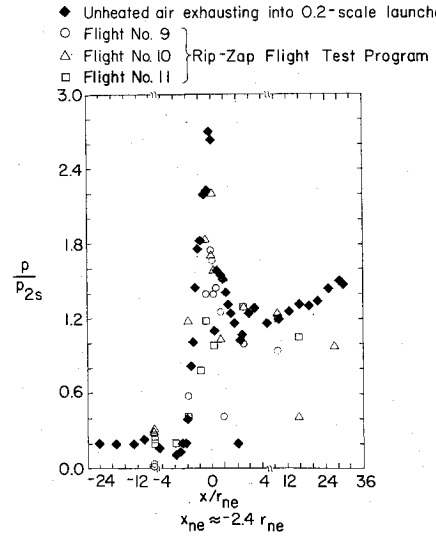

Fig. 6 A comparison of the Rip-Zap flight-test data with cold-gas data when the nozzle-exit plane was just upstream of the constriction.

behind a normal shock wave. As discussed previously, the pressures measured during the cold-gas tests were in good agreement with the theoretical values. This can be seen in Fig. 7, where the static wall pressure was approximately p_{t2} at the base of the forward-facing step and was approximately 0.5 p_{t2} (the value for sonic flow) near the exit plane of the aft tube. The flight-test measurements at the base of the constrictive step and near the exit plane of the aft tube did not agree as well with the theoretical values. The differences may be the result of the difficulty in obtaining flight-test measurements of the rapidly varying static wall pressure in the launcher and of possible differences between the actual value of γ for the flow in the launcher and that used in the theoretical solution. The differences between the theoretical and the flight-test values for the pressures downstream of the normal shock wave are similar to those observed downstream of the weak shock-wave system which occurred when the nozzle exhausted directly into the aft tube. Nevertheless, the pressure distributions from the rocket launchings were repeatable and considered to be in reasonable agreement with the flow model developed from the cold-gas tests.

The cold-gas test program conducted in the University's Rocket Exhaust Effects Facility included the constrictive area ratio as a controlled variable. The blow-by mass flow rate ($\dot{m}_{bb}$) for $p_{t1} \approx 950$ psia (6.55×10^6 N/m^2) is presented in Fig. 8 as a function of the nozzle-exit location. The blow-by flow rate was determined using a pitot probe located in the annular region between the simulated rocket and the launcher wall at the exit plane of the forward tube. Consider first the blow-by data for the launcher with $A_{aft} = 0.595\, A_{for}$, i.e., the 0.2-scale model of the Rip-Zap launcher, since the pressures for this launcher have been discussed. For -3 $r_{ne} < x_{ne} < 0$, the blow-by flow rates increased and then decreased as the nozzle-exit plane was moved past the step. The varying strength of the blow-by flow for these cold-gas tests appears to be similar to that indicated by the pressure data from the Rip-Zap flight tests, as discussed in Ref. 3. When the nozzle-exit plane had moved well into the forward tube, the exhaust flow was choked, and the blow-by flow rate was essentially constant (approximately 0.14 $\dot{m}_{ex}$). These data are qualitatively similar to those obtained during investigations of second-throat ejector-diffuser system. Panesci and German[7] found that "the location of the second-throat not only affects the starting pressure ratio but also can affect cell pressure if improperly located. When the second throat is positioned too far upstream, the free-jet impinges on the ramp, causing the cell pressure to increase. When a second throat is positioned too far downstream, the ejector will not start because of the decrease in Mach number entering the second throat." For $A_{aft} = 0.668\, A_{for}$, the experimentally determined pressure distributions were similar to those obtained for the 0.2-scale Rip-Zap launcher (which were presented in Fig. 4). As shown in Fig. 8, the blow-by mass flow rate ($\dot{m}_{bb}$) for the choked flow was approximately 10% of the mass flow rate through the nozzle ($\dot{m}_{ex}$). Empirical correlations developed by Jones et al.[8] and vertified by German et al.[9] indicate that second-throat ejector systems would be started for this area ratio. However, the launch-tube data clearly indicate that the flow downstream of the impingement shock was choked by the constriction, producing significant blow-by flow.

For $A_{aft} = 0.735\, A_{for}$, there was approximately 5% blow-by when the nozzle exhausted onto the constriction, i.e., $0 > x_{ne} > -5\ r_{ne}$. As the nozzle moved through the forward tube, i.e., for -11 $r_{ne} < x_{ne} < -5\ r_{ne}$, there was essentially no blow-by flow. The static wall pressures for these locations indicated that the exhaust flow remained supersonic even as it passed through the constriction and out the aft tube. However, when the nozzle was far removed from the step, i.e., $x_{ne} \leq -15\ r_{ne}$, the static wall pressure and the blow-by flow rates indicated the presence of a normal shock wave (i.e., the exhaust flow was choked). Thus, the data indicated that the combined effect of the displacement thickness of the viscous

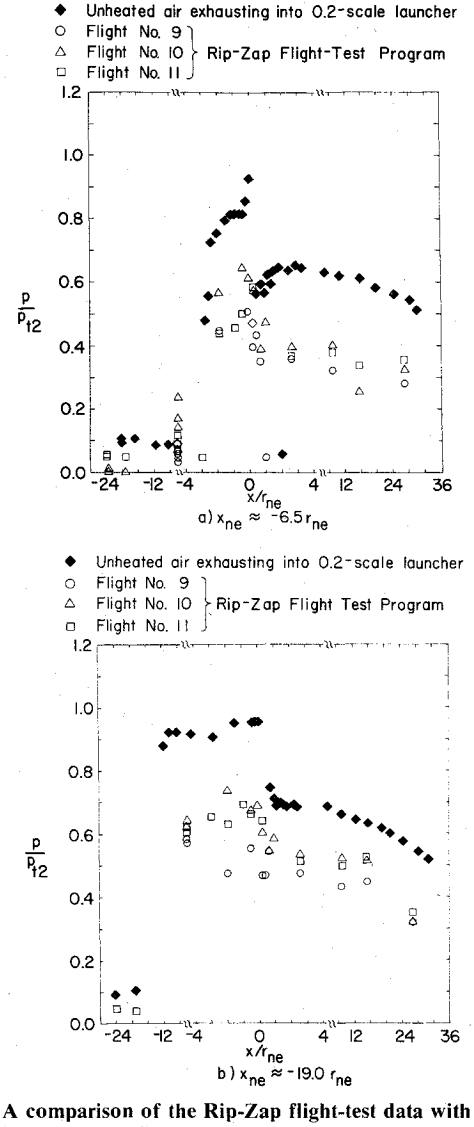

Fig. 7 A comparison of the Rip-Zap flight-test data with the cold-gas data for the choked flows.

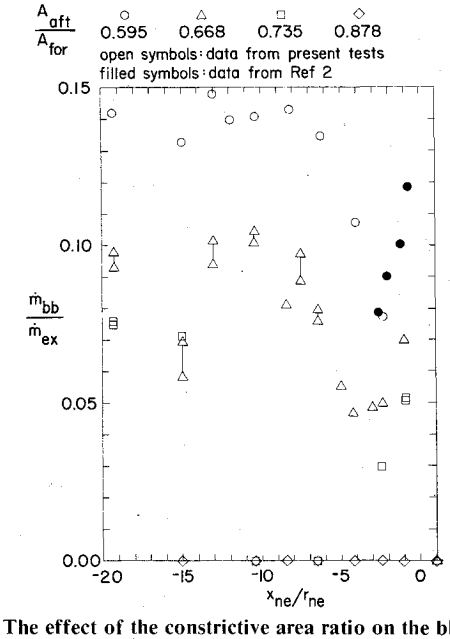

Fig. 8 The effect of the constrictive area ratio on the blow-by mass flow rate for the cold-gas tests.

flow and the constrictive step had become sufficient to choke the exhaust flow for this nozzle/launcher configuration. For $A_{aft} = 0.878\, A_{for}$, there was essentially no blow-by flow at any of the nozzle-exit locations tested, as is evident in Fig. 8.

The pressure measurements for PS1 (which was the first gage to be exposed to the rocket exhaust; see Fig. 2) in the Arrow flight-test program are presented in Fig. 9 as a function of the nozzle-exit position. Periodic pressure variations of the static wall pressure occurred during the interval when the nozzle exit plane was located between the orifice and the departure edge. The variations were due to reflections of the impingement shock wave in the fully supersonic flow. For comparisons with the data, the theoretical value of the static wall pressure downstream of the impingement shock (p_{2s}) is included. For this configuration, the theoretical value of p_{2s} was

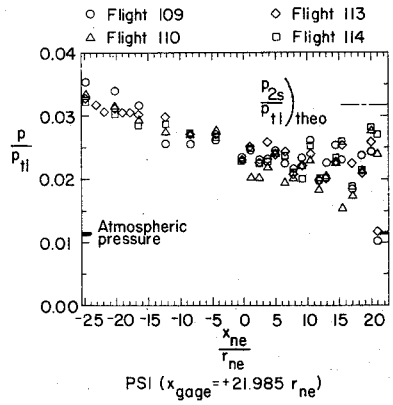

Fig. 9 The pressure history for PS1 in the Arrow flight-test program.

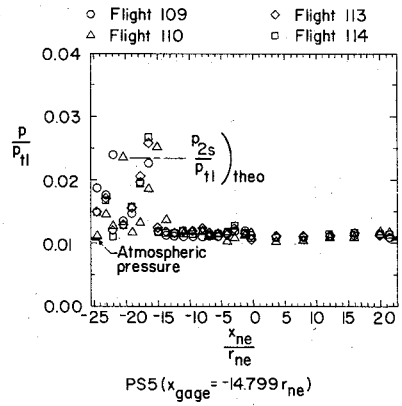

Fig. 10 Ths pressure history for PS5 in the Arrow flight-test program.

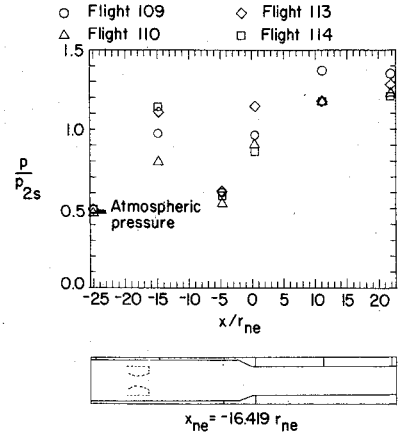

Fig. 11 The static wall-pressure distribution for the Arrow flight-test data.

in good agreement with the data, e.g., within 15% of the initial peak value for the measured pressure. The pressure recorded by PS1 rose for $x_{ne} < 0$, i.e., when the nozzle exit plane was in the forward tube.

The static-pressure history for PS5 (which was located in the large-diameter forward tube; see Fig. 2) for the Arrow flight-test program is presented in Fig. 10. A pulselike variation in the pressure measurements occurred as the rocket passed the constriction, i.e., for $-5\, r_{ne} < x < 0$. The relatively small magnitude of the pressure variation indicated that the mass flow rate for the blow-by flow generated as the exhaust impinged on the constriction was not significant. This conclusion was verified by photographs of the launchings. The pressure did not increase again until the nozzle had passed the orifice, at which time the impinging flow produced a sudden increase in pressure. The magnitude of the peak value was in reasonable agreement with the theoretical value downstream of an oblique shock. Furthermore, the oscillatory character of the pressures substantiated the conclusion that the flow remained supersonic. Thus, the exhaust flow for the Arrow configuration was not choked by the constriction, as had been the case for the Rip-Zap configuration.

The static pressures recorded by each of the six gages in the Arrow launcher when the nozzle-exit plane was 16.4 r_{ne} into the forward tube, i.e., $x_{ne} = -16.4\, r_{ne}$, were used to generate the pressure distribution presented in Fig. 11. Although there were only six gages, the pressure data clearly indicate that the impingement shock wave was a weak, oblique shock wave. As evidence of this, note the unity values for the dimensionless static pressures at PS5, which is the gage just downstream of the nozzle-exit plane. The fact that the pressure increased as the exhaust flow entered the aft tube indicates that the flow was supersonic along the entire length of the launcher. Whereas no significant blow-by flow was observed during these flight tests, significant blow-by flow was measured for some nozzle-exit positions for cold-gas flow into the launcher where $A_{aft} = 0.735\, A_{for}$ (near that of the Arrow launcher). The differences between the cold-gas simulation and the flight-test flowfield are attributed, in part, to differences in the growth of the boundary layer and, therefore, to differences in the viscous interactions. Furthermore, differences in the nozzle half-angle for the two nozzles and in the constrictive geometries also contributed to the choking of the cold-gas flow.

Concluding Remarks

Static wall-pressure measurements obtained when an underexpanded jet of unheated air was exhausted into a constrictive launch tube have been compared with similar data from flight-test programs. The cold-gas simulations not only provided a realistic flow model that could be used to interpret the flight-test data, but the cold-gas pressure measurements correlated reasonably well with the flight-test measurements. Based on the data obtained in these test programs, the following conclusions are made. One should, of course, use caution before extrapolating these results to radically different configurations.

1) The correlations between the cold-gas flows from a stationary nozzle and the exhaust flows from an accelerating rocket verify the assumption that the exhaust flow is quasisteady.

2) The effect of γ on the correlations could be reduced by dividing the static wall-pressure measurements by the theoretical value of the pressure downstream of the impingement shock wave.

Furthermore, the data obtained in these programs indicate that the constrictive area ratio A_{aft}/A_{for} was a dominant parameter in the generation of blow-by flow. For A_{aft}/A_{for} below a "critical value," the exhaust flow was choked by the constriction, and a large percentage of the exhaust flow was turned upstream. The critical value of the constrictive area ratio depends on many parameters, including those that

govern the impingement flow (i.e., the nozzle half-angle, the pressure and the Mach number in the nozzle-exit plane,the ratio r_{for}/r_{ne}, etc.) and the distance from the nozzle-exit plane to the constriction. This distance affects the flow properteries (e.g., Mach number and stagnation pressure) and the viscous layer thickness at the constriction. Variations in the constrictive geometry did not affect significantly the occurrence of the blow-by flow or the pressure distribution for the configurations studied. However, near the critical value of the constrictive area ratio, the constrictive geometry should become an important parameter, since it affects the character of the shock-wave system at the constriction and the resultant shock/boundary-layer interaction.

References

[1]"Feasibility Flight Testing of Rocket Impelled Projectile (RIP)," LTV Aerospace Corporation, Michigan Div. 7-52100/3R-5, May 1973.

[2]Bertin, J.J., Horn, M.K., and Webber, T.K., "Experimental Study of Flow Field Produced When an Underexpanded Jet Exhausts into a Constrictive Stepped Launch Tube," The University of Texas at Austin, Aerospace Engineering Rep. 74002, Jan. 1974.

[3]Bertin, J.J. and Batson, J.L., "The Experimentally Determined Rocket-Exhaust Flow Field in a Constrictive Tube Launcher," *Journal of Spacecraft and Rockets*, Vol. 12, Dec. 1975, pp. 711-717.

[4]Shapiro, A.H., *The Dynamics and Thermodynamics of Compressible Fluid Flow*, Ronald Press, New York, 1953.

[5]Ames Research Staff, "Equations, Tables, and Charts for Compressible Flow," NACA Rep. 1135, 1953.

[6]Batson, J.L. and Bertin, J.J., "Experimental Study of Flow Field Produced When an Underexpanded Rocket Exhausts into Cylindrical Tube," AIAA Paper 73-1227, Las Vegas, Nov. 1973.

[7]Panesci, J.H. and German, R.C., "An Analysis of Second-Throat Diffuser Performance for Zero-Secondary-Flow Ejector Systems," TDR-63-249, Dec. 1963. Arnold Engineering Development Center, Arnold AFB, Tenn.

[8]Jones, W.L., Price, H.G., Jr., and Lorenzo, C.F., "Experimental Study of Zero-Flow Ejectors using Gaseous Nitrogen," NASA TND-203, March 1960.

[9]German, R.C., Bauer, R.C., and Panesci, J.H., "Methods for Determining the Performance of Ejector-Diffuser Systems," *Journal of Spacecraft and Rockets*, Vol. 3, Feb. 1966, pp. 193-200.